Micro-Raman study of isotope substitution in $YBa_2Cu_3{}^{18}O_{6.2}$ during local laser annealing

V. G. Ivanov and M. N. Iliev
Faculty of Physics, University of Sofia, BG-1126 Sofia, Bulgaria

C. Thomsen
Institut für Festkörperphysik, Technische Universität Berlin, Hardenbergstrasse 36, D-10623 Berlin, Germany
(Received 16 March 1995; revised manuscript received 11 July 1995)

The local laser heating of $YBa_2Cu_3{}^{18}O_{6.2}$ in air was used to study the oxygen diffusion and oxygen ordering in sample volumes of the order of a few μm^3. Raman microprobe at points corresponding to different annealing temperatures was applied to monitor both the stages of substitution of ^{16}O for ^{18}O at different oxygen sites and the structural changes in the basal [Cu(1)-O(1)] planes occurring during the oxygen in-diffusion. The population of the O(1) sites initially results in the formation of short Cu(1)-O(1) fragments which later conjunct into long chains. The results can be applied for a better understanding of oxygen reordering processes in $YBa_2Cu_3O_{7-\delta}$ during thermal treatment.

I. INTRODUCTION

The oxygen atoms in $YBa_2Cu_3O_{7-\delta}$ (YBCO) occupy four inequivalent positions: O(1) (in the Cu-O chains), O(2),O(3) (in the Cu-O planes), and O(4) (apex oxygen), and contribute in a different way to the electronic, vibrational, etc., properties of the material. The O(2), O(3), and O(4) sites are always filled. The population of the O(1) sites depends on the growing and treatment conditions (in particular on the thermal annealing at different atmospheres or vacuum) and may vary between 0, as in tetragonal $YBa_2Cu_3O_6$ ($\delta=1$), and 1, as in orthorhombic $YBa_2Cu_3O_7$ ($\delta=0$). It is commonly accepted that the Cu(1)-O(1) chains serve as reservoirs for excess holes.[1] At $\delta>0.5$ the holes are localized at the chains and do not contribute to the conductivity at low temperatures. At $\delta\leq 0.5$, a hole transfer occurs to the Cu(2)-O(2),O(3) planes and the samples become superconducting.

Local laser annealing of oxygen-rich YBCO films in vacuum (inert atmosphere) or of oxygen-deficient YBCO films in oxygen atmosphere has recently been applied in "laser writing" technology to produce nonsuperconducting strips on a superconducting substrate and *vice versa*.[2] While obviously the basic effect of laser treatment is in- or out-diffusion of oxygen, the physical processes at a microlevel and their spacial distribution within and near the irradiated area are still not investigated in detail. The laser heating differs from the homogeneous thermal annealing by the existence of strong temperature gradients and a rapid temperature decrease after irradiation. Similarly to the case of "rapid quenching," the latter may result in freezing the laser-heating-induced structural disorder in the Cu(1)-O(1) planes followed by "room-temperature-annealing" reordering processes.[3,4]

Raman spectroscopy allows one to observe directly the atomic vibrations and to probe the local site coordination. The frequencies, polarization properties, and the resonant behavior of the Raman-allowed phonons expected for disorder-free $YBa_2Cu_3O_7$ and $YBa_2Cu_3O_6$ structures are well established.[5] The origin of many additional spectral features, most strongly pronounced in poorly oxygenated, doped, or mixed $YBa_2Cu_3O_{7-\delta}$ samples, however, is either unclear or controversially discussed. Nevertheless, there is a general agreement that the additional lines in the Raman spectra (if not from "impurity" phases) are due to local changes of the atomic enviroments resulting in activation of otherwise Raman-forbidden modes.[6–8]

A Raman microprobe was recently applied to study the nature of local laser-irradiation-induced structural changes and their spacial distribution within the area of oxygen-rich $RBa_2Cu_3O_{7-\delta}$ (R = Nd,Y) irradiated in air.[9] It was established that the laser annealing, resulting in this case in a reduction of the oxygen content ($0<\delta<0.5$), strongly modifies the Raman band assigned to vibration along the c axis of the O(4) atoms. It develops into a complex line shape that could be interpreted as a superposition of components related to coexisting ortho-I and ortho-II microstructures.[10] The oxygen content and the relative weight of the ortho-II microstructures vary with the irradiation dose. In consistence with an earlier suggestion of Wake *et al.*,[8] the Raman line appearing after irradiation at 600 cm^{-1} for "Nd123" and at 596 cm^{-1} for "Y123" was assigned to vibrations of O(1) atoms at the ends of the b-axis-oriented chain fragments, which become Raman active due to loss of inverse symmetry of the O(1) sites.

The assignment of a "defect" oxygen mode to O(1)[O(5)], O(4) or O(2),O(3) vibration(s) can be made unambiguous by observing the change of the mode frequency after a site selective $^{18}O \leftrightarrow {}^{16}O$ isotopic substitution. Cardona *et al.*[11] and later Conder *et al.*[12] have performed selective isotopic substitution experiments at (i) only the O(1) sites, (ii) the O(1) and O(4) sites, and (iii) all oxygen sites. It was shown in Ref. 12 that for samples of weight 100–150 mg, the time required to obtain complete isotopic exchange of O(1), or O(1) and O(4) varied between 1 day and 1 month. Given that the volume for atomic exchange in our irradiated spot is small, however, the time for completing the process will be much shorter.

There are several reports on the $^{18}O \leftrightarrow {}^{16}O$ isotope effect on the ir and Raman frequencies of $YBa_2Cu_3O_{7-\delta}$ and also on T_c.[11,13–15] In particular, it has been shown that Raman

spectroscopy is a relevant tool for determining the degree of isotopic substitution at the O(4) and O(2),O(3) sites from the frequency of the A_g modes at $\approx$ 500 and at 440 or 335 cm^{-1}, respectively.

In this work we show on the example of $YBa_2Cu_3{}^{18}O_{6.2}$ that it was possible by local laser heating in air to substitute site-selectively ^{16}O for ^{18}O in volumes of the order of a few μm^3, the duration of the laser irradiation being of the order of 5–15 min. By Raman microprobe at points corresponding to different irradiation doses we were able to monitor all stages of isotopic substitution [(i), (ii), and (iii)] as well as to follow the structural changes in the basal [Cu(1)-O(1)] planes during the oxygen in-diffusion. In particular, the appearance of the Raman-forbidden lines at 248 cm^{-1} and 596 cm^{-1} and their evolution with oxygen content (irradiation dose) provide evidence for conjunction of the short Cu(1)-O(1) fragments into long chains.

II. SAMPLE AND EXPERIMENT

We used a ceramic sample of $YBa_2Cu_3{}^{18}O_{6.2}$, prepared following a procedure described in Ref.13. The visual observation under a microscope (in polarized light) of the polished surface of the pellet showed that the typical size of the microcrystals constituting the sample was 2 to 20 μm. The laser heating in air was performed by focussing an Ar^+ laser beam (λ_L= 488 nm) through the 50× objective of an optical microscope in a spot of diameter 3−5 μm on a single microcrystal. The averaged incident laser power at the sample varied between 5 and 15 mW, and irradiation lasted from 5 to 15 min. The irradiated spot became slightly brighter indicating change of the oxygen content. The Raman spectra were probed using the triple multichannel spectrometer Microdil 28 equipped with a microscope and a precise XY scanning system. The same laser line was used for excitation at much lower power (0.5 to 1 mW). The 100× objective of the microscope was used to focus the incident beam in a spot of $\sim 1\,\mu m$ diameter and to collect the scattered light. The scanning system allowed to scan the crystal surface by 0.1 μm steps with 0.1 μm reproducibility at a distance of 1 mm. The typical acquisition time for one spectrum was 5000 sec. The Raman spectra were taken at room temperature, and at least 24 h after the thermal treatment.

III. THERMODYNAMIC CONDITIONS DURING LASER ANNEALING

The rate of oxygen in- or out-diffusion, as well as the isotope exchange kinetics depend strongly on the temperature in the exchange volume. To interpret the experimental data we present model calculations of the temperature distribution within the irradiated crystal during laser annealing.

In the visible range (in our case λ_L=488 nm) the light penetration depth does not exceed 1000 Å . Since we are interested in temperature profiles in the scale of few μm, it is reasonable to assume that the laser power is absorbed at the crystal surface and there are no heat sources in the bulk. In this case, the heat transport equation in the depth of the crystal simplifies to

$$\Delta T(\mathbf{x})=0, \tag{1}$$

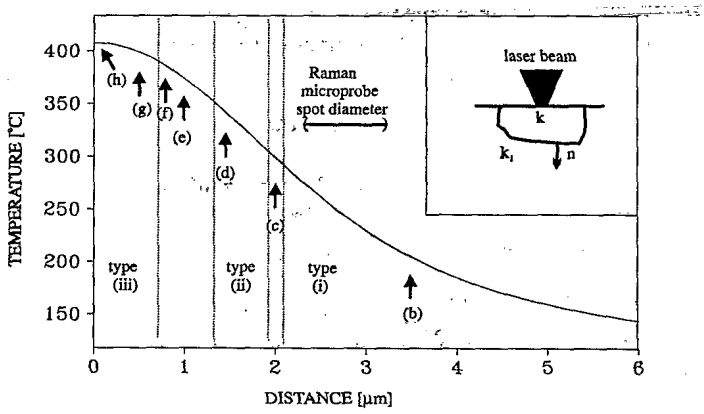

FIG. 1. Distribution of the temperature during laser annealing with P_L=11 mW with laser beam with Gaussian radius $\approx$1.5 μm. The ranges of distances corresponding to the types (i), (ii), and (iii) isotopic exchange as well the distances corresponding to the micro-Raman spectra of Fig. 2 are also indicated. The inset shows schematically the laser annealing configuration.

where Δ is the Laplace operator. The boundary condition at the illuminated surface takes the form

$$-k\frac{\partial T}{\partial z}=\frac{(1-R)P}{2\pi\sigma^2}\exp\left(-\frac{r^2}{2\sigma^2}\right), \tag{2}$$

where R is the reflectivity of the surface; P, the incident laser power; σ, the Gaussian radius of the spot at the surface. The thermal conductivity k is assumed to be isotropic. The origin of the coordinate system is at the center of the irradiated spot, with Cartesian axes X and Y parallel to the surface ($r=\sqrt{x^2+y^2}$), and Z pointing to the depth of the crystal. This equation also implies that all absorbed heat flows through the contacts of irradiated crystal with the neigboring crystals, and the heat losses through the illuminated surface (due to thermal radiation and air convection) can be neglected.

In order to obtain a unique solution of Eq. (1) with boundary condition (2) one has to specify the boundary conditions at these parts of the crystal surface, which are not exposed to laser radiation. For a crystal that is large compared to the radius of the laser spot, it is plausible to take as a starting approximation the temperature distribution corresponding to a semi-infinite layer with ambient temperature (T_{amb}=23 °C in our case) at infinite distance from the $\mathbf{x}$ = 0 point. The problem has been solved by Lax,[16] and the result for the temperature rise with respect to T_{amb} is given by:

$$T^{(0)}(r,z)=T^{(0)}_{max}\sqrt{\frac{2}{\pi}}\int_0^\infty \exp[-(\lambda^2/2+\lambda z/\sigma)]J_0(\lambda r/\sigma)d\lambda, \tag{3}$$

$$T^{(0)}_{max}=(1-R)P/(k\sigma\sqrt{8\pi}). \tag{4}$$

In order to account for the effects of finite size on the temperature distribution let us consider the illuminated crystal as embedded in a homogeneous effective medium with thermal conductivity $k_1=k-\delta k$, equal to the macroscopic thermal conductivity of the ceramics (see the inset of Fig. 1).

At the interface between the crystal and its surrounding, the normal derivative of the temperature undergoes a jump, according to the equation:

$$k(\nabla_n T)_{\text{crystal}} = k_1(\nabla_n T)_{\text{medium}}. \tag{5}$$

Considering δk as a small perturbation, the first order correction to the temperature inside the crystal is given by the expression

$$T^{(1)}(\mathbf{x}) = -\frac{\delta k}{k}\oint_S \frac{\nabla_n T^{(0)}}{4\pi|\mathbf{x}-\mathbf{x}'|}dS'. \tag{6}$$

The integration is over the closed surface, composed by the interface between the crystal and its surrounding plus its mirror image with respect to the illuminated surface. The function $T^{(1)}(\mathbf{x})$ varies relatively moderately inside S, which results in a nearly constant rise of the temperature, given by the expression

$$T^{(1)} = T^{(0)}_{\max}\frac{\sigma}{L}\sqrt{\frac{2}{\pi}}, \tag{7}$$

where L is a characteristic size of the crystal. The temperature inside the crystal is given by

$$T(\mathbf{x}) = T_{\text{amb}} + T^{(0)}(\mathbf{x}) + T^{(1)}(\mathbf{x}). \tag{8}$$

Since the final result depends on $1/k$, we take for k the harmonic averaged value of k_c, k_a, and k_b, using the literature values $k_c = 2$ Wm^{-1} K^{-1} and $k_a = k_b = 8$ Wm^{-1} K^{-1} from Ref. 17. The so-estimated averaged value is $k = 4$ Wm^{-1} K^{-1}. The data refer to $T = 300$ K, but we can extrapolate them to higher temperatures, taking into account the relatively slow variation of thermal conductivity above ≈ 150 K.[17] The thermal conductivity of the ceramics is lower than the one of a single crystal, because of voids between grains and additional thermal resistance at the intergrain contacts. Following published data[18] we accept $\delta k \approx 1/2k$. For the reflectance coefficient R we take the value 0.13.[19]

In Fig. 1 is shown the radial distribution of the annealing temperature on the illuminated surface of the crystal, used to obtain the Raman spectra described in Sec. IV. The incident laser power during annealing was 11 mW with Gaussian radius $\approx 1.5\mu$m. In the calculation of finite size correction, a model of semispherical grain of radius 6 μm was considered.

Several implications can be made from Fig. 1. At the center of irradiated area the temperature exceeds 400 °C which is sufficient to initiate oxygen diffusion, as well as isotopic exchange in all oxygen sites.[12] Experimental studies of δ versus T dependence[20] show that at this temperature, and for oxygen partial pressure in air of ≈ 0.2 bar, the equilibrium oxygen content in YBCO samples is 6.7–6.8. This means that during laser heating oxygen in-diffusion will prevail, thus increasing the total oxygen content of the annealed volume. Of course, the final oxygen content at a given distance from the center of irradiated area will be smaller than the equilibrium value, depending both on the annealing time and local temperature.

It follows from Fig. 1 that far from the center of irradiated spot, the annealing temperature drops below 200 °C. The latter implies that by applying Raman microprobe at different points within the irradiated area we can study the different stages of isotopic exchange,[12] namely, above 398 °C, the type (iii) (all sites) exchange; between 307 °C and 353 °C, the type (ii) (apex + chains); and bellow 290 °C, the type (i) (only chains). The corresponding ranges of distances are indicated in Fig. 1.

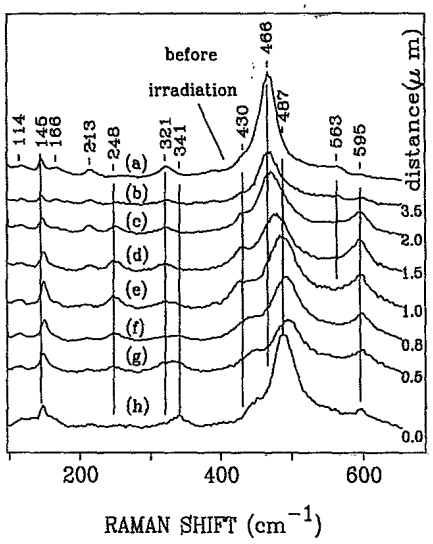

FIG. 2. Raman spectra of $YBa_2Cu_3{}^{18}O_{6.2}$ before irradiation [spectrum (a)] and after irradiation [spectra (b)–(h)]. The numbers correspond to the distance (in μm) from the center of the irradiated spot.

As several approximations were used in our model, its quantitative predictions should not be taken as letterperfect ones. However, the experimental results described in Sec. IV confirm also qualitatively the conclusions drawn above. More rigorous treatment of heat transport can be made in the case of thin film samples. A detailed study of laser heating of thin films of YBCO on MgO substrates has recently been performed by Bock.[21]

IV. RESULTS AND DISCUSSION

In Fig. 2, (b)–(h) are shown the Raman spectra collected under the same experimental conditions from a microcrystal of unknown orientation at different distances from the center of the irradiated area. The temperatures during laser annealing at points where the Raman spectrum was probed can be extracted from temperature profile in Fig. 1. Spectrum (a) was measured at the center before irradiation. It is identical to the spectra measured after irradiation at points far enough from the center ($d > 5\mu$m). A comparison with the spectra taken from another (ab-oriented) microcrystal (not shown here) allowed us to determine the Raman line polarizations.

For a better understanding of the laser-heating-induced changes let us first analyze the Raman spectrum (a) taken before irradiation. The weak line at 114 cm^{-1} and the mainly xx-polarized line at 145 cm^{-1} can be assigned unambiguously to the A_{1g} vibrations of Ba and Cu(2), respectively. The origin of the weak lines at ~ 166 cm^{-1} and 214 cm^{-1} (zz polarized) is less clear. The frequency of the latter peak is close to that of the Raman-forbidden B_{1u} mode involving mainly vibrations of Y. It has been shown in hydrogenated

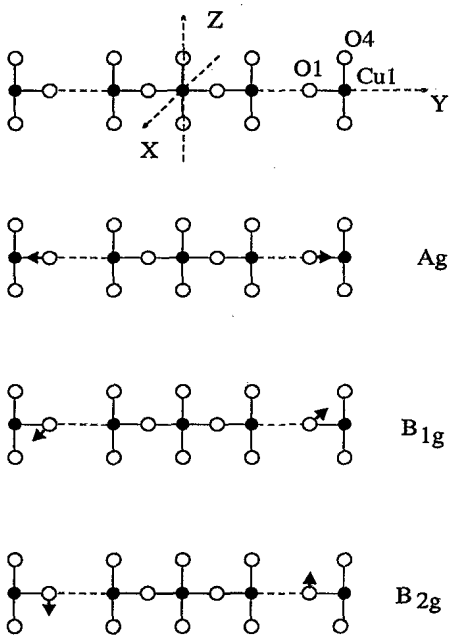

FIG. 3. Raman active modes of $[Cu(1)]_n[O(4)]_{2n}[O(1)]_{n-1}$ chain fragment involving displacements of O(1) atoms. The Cu(1) Raman modes are of the same symmetries and involve Cu(1) displacements in the same directions. The Cu atoms are grey, O is white.

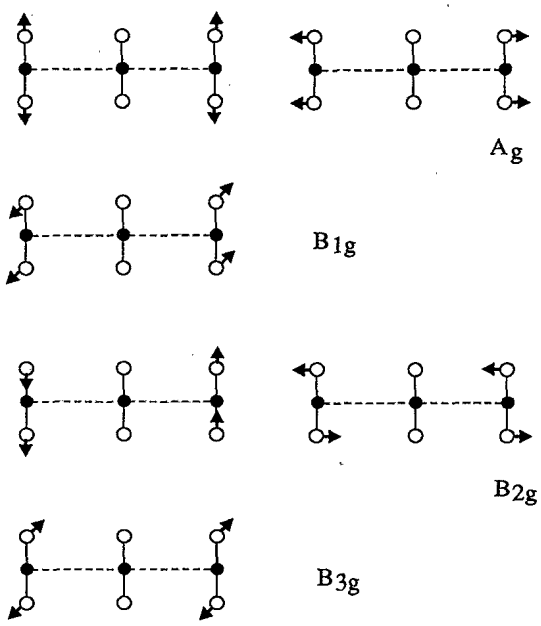

FIG. 4. Raman active modes of $[Cu(1)]_n[O(4)]_{2n}[O(1)]_{n-1}$ chain fragment involving displacements of apex O(4) atoms.

$YBa_2Cu_3O_{7-\delta}$ (Ref. 22) that local disorder may activate this mode in the Raman spectrum with the same zz polarization. The possibility of this mode being of E_g type and related to O(4) vibrations along the b axis, may be ruled out for two reasons: the Raman line of E_g symmetry corresponding to the orthorhombic B_{2g} at ~ 210 cm^{-1} has not been found for $\delta \leq 0.5$,[23] and, more importantly, in the ^{18}O for ^{16}O substituted samples the E_g frequency is expected near 200 cm^{-1} rather than at 214 cm^{-1} as it is seen in Fig. 2.

The Raman lines in the frequency range above 300 cm^{-1} correspond to vibrations of the light oxygen atoms. For the nonisotopically substituted $YBa_2Cu_3{}^{16}O_{6.2}$ the most pronounced modes[24] are those of the O(2)-O(3) out-of-phase vibrations (B_{1g} symmetry) at 340 cm^{-1}, O(2)-O(3) in-phase vibrations (A_{1g}) at 450 cm^{-1}, and the O(4) vibrations (A_{1g}) at 475–480 cm^{-1}. The observation of the Raman lines in our sample corresponding to the O(2),O(3) vibrations at 322 and 428 cm^{-1} indicates an almost complete substitution of ^{18}O for ^{16}O at the O(2) and O(3) sites, while the appearance of the apex-oxygen line at 465 cm^{-1} is likely to be due to incomplete isotopic substitution at the O(4) sites. Alternatively it has been hypothesized that the lower isotopic shift of apex-oxygen line may be due to an anharmonic potential.[14] The assignment of the line at 563 cm^{-1} will be discussed below.

The main changes in the spectra (b) and (c), when compared to (a), is the appearance and enhancement of the lines at 248 and 596 cm^{-1}, whereas the line at 563 cm^{-1} disappears. As follows from model calculations, at these distances the annealing temperature is well below 300 °C. Therefore, the observed modification of the spectrum could be due to activated diffusion and isotopic exchange only in the basal planes. Indeed the changes occur before the onset of the frequency shift of the apex and plane-oxygen bands. It is plausible to assume that 248 and 596 cm^{-1} peaks correspond to vibrations, which become visible due to disorder in the basal planes—namely the presence of copper-oxygen chain fragments of finite length.

Any finite copper-oxygen chain $[Cu(1)]_n[O(4)]_{2n}[O(1)]_{n-1}$ (or shorter Cu_nO_{3n-1}, $n \geq 2$) is invariant with respect to the symmetry group D_{2h} (Fig. 3). The group-theoretical analysis of vibrations of a finite Cu_nO_{3n-1} linear fragment shows that any pair of equivalent Cu(1) or O(1) atoms, which are not in the inversion center of the fragment, participates in six modes:

$$A_g+B_{1g}+B_{2g}+B_{1u}+B_{2u}+B_{3u},$$

three of them being Raman active. The directions of atomic displacements, uniquely determined from symmetry considerations, are presented at Fig. 3. Any group of four equivalent O(4) atoms, which are not in the symmetry axis z gives rise to 12 modes:

$$2A_g+B_{1g}+2B_{2g}+B_{3g}+A_u+2B_{1u}+B_{2u}+2B_{3u}.$$

Corresponding displacement patterns of the Raman-active modes are shown in Fig. 4.

Because of its high frequency, the 596 cm^{-1} mode can be assigned unambiguously to oxygen vibrations, involving mainly stretching of Cu-O bonds. There are three types of such stretching vibrations: the A_g mode of O(1) and one B_{2g} and one A_g modes of O(4). The A_g mode of O(4) is already present in the spectrum of the ideal stochiometric "123" structure, giving rise to the apex band at ≤ 500 cm^{-1}. The B_{2g} vibrations should be observable in xz-scattering configuration and are generally found to be very weak in the high T_c's.[25,26] Therefore, the only candidate for

the 596 cm^{-1} band, which is both of stretching type, and has diagonal Raman tensor, is the A_g vibration of O(1) atoms along the y axis (Fig. 2). Such an assignment is supported by the fact that the frequency of the Raman-allowed vibrations[27] of oxygen atoms of the double Cu-O chains of the "124" compound $YBa_2Cu_4O_8$ is 605 cm^{-1}.

The corresponding stretching vibration of the chain copper in the 124 system has a frequency of 250 cm^{-1}. Thus is it reasonable to accept that the 248 cm^{-1} line in our spectra corresponds to A_g vibrations of Cu(1) atoms near the free chain ends along the y axis.

As the frequency ratio of the 563 cm^{-1} and 596 cm^{-1} lines is equal to the square root of the masses of ^{16}O and ^{18}O, there is little doubt that they are the ^{18}O and ^{16}O counterparts of the same otherwise Raman-forbidden O(1) mode, respectively. A certain number of short chain fragments are therefore present already in the starting material.

Spectra (d) and (e), corresponding to points at 1.5 and 1.0 μm from the center, respectively, are characterized by saturation of the 248 and 596 cm^{-1} Raman line intensities, whereas the line at 213 cm^{-1} is strongly reduced. The apex-oxygen line broadens and its maximum shift up to 487 cm^{-1}. An inspect of the temperature profile (Fig. 1) shows that at points (d) and (e), the annealing temperature is high enough to activate isotope exchange at apex positions. This can partly account for the upward shift of the frequency of O(4) vibrations. An additional hardening of the mode may come from increase of the oxygen content of the basal planes, due to prevailing oxygen in-diffusion.

The spectra (f) and (g), from points at 0.8 and 0.5 μm from the center, respectively, as well as the spectrum (h) taken at the center of the irradiated spot, represent the case of a substitution of ^{16}O for ^{18}O at all oxygen sites [type (iii)]. Indeed, the Raman lines corresponding to the out-of-phase and in-phase vibrations along c of the O(2),O(3) atoms shift to the frequencies 341 and 435 cm^{-1}, which are characteristic for $YBa_2Cu_3{}^{16}O_{7-\delta}$. It is remarkable that although in the spectra (f) and (g) the apex-oxygen frequency slightly increases (a signature for higher oxygen content), the relative intensity of the Raman-forbidden lines at 248 and 596 cm^{-1} slightly decreases. At the center itself [spectrum (h)] the 248 cm^{-1} line is totally suppressed, whereas the one at 596 cm^{-1} is very weak. At the center one also observes strong enhancement of the apex oxygen peak which becomes narrower and shifts down slightly to its ortho-II position (487 cm^{-1}).

The broadening of the apex-oxygen band in the spectra (d)–(g) can be understood given ordered microstructures with different oxygen content coexist in the scattering volume. It has been shown that a frequency of ~487 cm^{-1} is characteristic for the O(4) vibrations along c in an Ortho-II phase-like surrounding.[4,10] A relatively big amount of microdomains of higher oxygen content (e.g., like in ortho-I or ortho-III phases) can give rise to additional high-frequency component(s), thus accounting for the higher apex-oxygen frequency in the spectra (f) and (g).

The experimental results on the laser annealing of oxygen-deficient $YBa_2Cu_3O_{7-\delta}$ presented above can be described consistently as follows. At low laser irradiation doses (annealing temperatures) the in- and out-diffusion of oxygen is restricted to the Cu(1)-O(1) planes. As the in-diffusion rate prevails, the O1 content increases ($\delta > 0.6$) and short Cu(1)-O(1) fragments are formed. At higher irradiation doses there is further in-diffusion of oxygen which rather joins already existing Cu(1)-O(1) chains than forming new ones [the intensities of the 248 cm^{-1} and 596 cm^{-1} lines related to the atoms Cu(1) and O(1) at the fragment end remain nearly unchanged]. Simultaneously, a mutual exchange of O(1) $\leftrightarrow$ O(4) takes place. At the highest doses the oxygen diffusion involves all oxygen sites [O(1) $\leftrightarrow$ O(4) $\leftrightarrow$ O(2),O(3)]. At these temperatures the in- and out-diffusion rates become equal and the oxygen content of the sample saturates at the value ~6.5($\delta \sim 0.5$). The number of chain fragments, and hence of the Raman active Cu(1) and O(1) end atoms, decreases in favor of a formation of long chains. The resulting local structure is of the ortho-II type. It is not clear, however, whether the structure is coherent at long distances.

In conclusion, it was shown in this study that depending on the laser irradiation dose different types of oxygen diffusion and oxygen reordering take place. Local laser annealing results in a spacial distribution of the oxygen content and local oxygen structures. The assignment of the 248 cm^{-1} and 596 cm^{-1} defect Raman lines to the Cu(1) and O(1) vibrations of the end of Cu(1)-O(1) fragments was verified. Thus, these lines could be used as markers for existence of short Cu(1)-O(1) chains. We believe that our results lead to a better understanding of the physical processes during laser annealing, already applied in the novel technology of laser patterning of YBCO thin films.[2]

ACKNOWLEDGMENTS

Numerous fruitful discussions with V. Hadjiev are highly appreciated. The work was supported by the Bulgarian National Science Fund (Contract No. F410/94) and the Commission of EU (CIPA-CT93-0032).

[1] R. J. Cava, B. Batlogg, K. M. Rabe, E. A. Rietman, P. K. Gallagher, and L. W. Rupp, Jr., Physica C **156**, 523 (1988).

[2] R. Sobolewski, W. Xiong, and W. Kula, IEEE Trans. Appl. Supercond. **3**, 2986 (1993).

[3] B. W. Veal, A. P. Paulikas, H. You, H. Shi, Y. Fang, and J. W. Downey, Phys. Rev. B **42**, 6305 (1990).

[4] V. G. Hadjiev, C. Thomsen, J. Kircher, and M. Cardona, Phys. Rev. B **47**, 9148 (1993).

[5] C. Thomsen, in *Light Scattering in High-T_c Superconductors*, edited by M. Cardona and G. Güntherodt, Topics in Applied Physics Vol. 68 (Springer-Verlag, Berlin, 1991), pp. 285–359.

[6] C. Thomsen, M. Cardona, B. Gegenheimer, R. Liu, and A. Simon, Phys. Rev. B **37**, 9860 (1988).

[7] K. F. McCarty, J. C. Hamilton, R. N. Shelton, and D. S. Ginley, Phys. Rev. B **38**, 2914 (1988).

[8] D. R. Wake, F. Slakey, M. V. Klein, J. P. Rice, and D. M. Gins-

berg, Phys. Rev. Lett. **67**, 3728 (1991).
[9] V. G. Ivanov, V. G. Hadjiev, and M. N. Iliev, Physica C **235–240**, 1255 (1994).
[10] M. Iliev, C. Thomsen, V. Hadjiev, and M. Cardona, Phys. Rev. B **47**, 12 341 (1993).
[11] M. Cardona, R. Liu, C. Thomsen, W. Kress, E. Schönherr, M. Bauer, L. Genzel, and W. König, Solid State Commun. **67**, 789 (1988).
[12] K. Conder, E. Kaldis, M.Maciejewski, K. A. Müller, and E. F. Steigmeier, Physica C **210**, 282 (1993).
[13] C. Thomsen, E. Schönherr, B. Friedl, and M. Cardona, Phys. Rev. B **42**, 943 (1990).
[14] G. Ruani, C. Taliani, M. Muccini, K. Konder, E. Kaldis, H. Keller, D. Zech, and K. Alex Müller, Physica C **226**, 101 (1994).
[15] D. Zech, H. Keller, K. Konder, E. Kaldis, E. Liarokapis, N. Poulakis, and K. A. Müller, Nature **371**, 681 (1994).
[16] M. Lax, J. Appl. Phys. **48**, 3919 (1977).
[17] S. J. Hagen, Z. Z. Wang, and N. P. Ong, Phys. Rev. B **40**, 9389 (1989).
[18] A. Jezowsci, J. Mucha, K. Rogacki, R. Horyn, Z. Bukowski, M. Harobowski, J. Rafalowicz, J. Stepien-Damm, C. Sulkowski, E. Trojnar, A. J. Zaleshi, and J. K. Klamum, Phys. Lett. A **122**, 4311 (1987).
[19] W. Marcowitsh, W. Mayr, P. Scwab, and X. Z. Wang, Physica C **233**, 117 (1994).
[20] K. Conder, J. Karpinski, E. Kaldis, S. Rusiecki, and E. Jilek, Physica C **196**, 164 (1992).
[21] A. Bock, Phys. Rev. B **51**, 15 506 (1995).
[22] V. G. Hadjiev, M. V. Abrashev, M. N. Iliev, and L. N. Bozukov, Physica C **171**, 257 (1990).
[23] V. G. Hadjiev, C. Thomsen, and M. Cardona, in *Proceedings of the 13th International Conference on Raman Spectroscopy*, Würzburg, 1992, edited by W. Kiefer, M. Cardona, G. Schaack, F. W. Schneider, and H. W. Schrötter (John Wiley & Sons, Chichester, 1992), p. 878.
[24] M. N. Iliev and V. G. Hadjiev, J. Phys. Condens. Matter **2**, 3135 (1990).
[25] K. F. McCarty, J. Z. Liu, R. N. Shelton, and H. B. Radousky, Phys. Rev. B **41**, 8792 (1990).
[26] B. Friedl, C. Thomsen, E. Schönherr, and M. Cardona, Solid State Commun. **76**, 1107 (1990).
[27] E. T. Heyen, R. Liu, C. Thomsen, R. Kremer, M. Cardona, J. Karpinski, E. Kaldis, and S. Rusiecki, Phys. Rev. B **41**, 11 058 (1990).